Applied Physics Letters

Electro-chemo-mechanical coupling of nanoporous gold at the microscale

Cite as: Appl. Phys. Lett. **115**, 251602 (2019); https://doi.org/10.1063/1.5128049
Submitted: 16 September 2019 . Accepted: 03 December 2019 . Published Online: 17 December 2019

Yijuan Wu, Jürgen Markmann, and Erica T. Lilleodden

Applied Physics Letters ARTICLE scitation.org/journal/apl

Electro-chemo-mechanical coupling of nanoporous gold at the microscale

Cite as: Appl. Phys. Lett. **115**, 251602 (2019); doi: 10.1063/1.5128049
Submitted: 16 September 2019 · Accepted: 3 December 2019 ·
Published Online: 17 December 2019

Yijuan Wu,[1,a)] Jürgen Markmann,[1,2] and Erica T. Lilleodden[1,3]

AFFILIATIONS

[1]Institute of Materials Research, Materials Mechanics, Helmholtz-Zentrum Geesthacht, Max-Planck-Straße 1, 21502 Geesthacht, Germany
[2]Institute of Materials Physics and Technology, Hamburg University of Technology, Eißendorferstr. 42, 21073 Hamburg, Germany
[3]Institute of Advanced Ceramics, Hamburg University of Technology, Denickestr. 15, 21073 Hamburg, Germany

[a)]**Author to whom correspondence should be addressed:** yijuan.wu@hzg.de

ABSTRACT

The observation of reversible strengthening and stiffening of nanoporous gold (NPG) under electrochemical potential has opened opportunities to exploit this material for multifunctional applications. Yet the complex structural geometry and length-scales involved make a definitive understanding of structural correlations to the behaviors difficult at best. Achievement of coupled electro-chemo-mechanical testing at the micrometer scale is a key step toward this goal. Here, we introduce an experimental approach to investigate the elastic and plastic behaviors of NPG under electrochemical potential at the microscale using a modified nanoindentation setup and multiple load function. The *in situ* experiments in electrolyte show a significant increase by 32% in strength of pillars in a positive potential regime where oxygen adsorption occurred. This response was found to be reversible, which agrees with macroscopic results, while the elastic modulus was shown to be insensitive to the applied potential—an observation inconsistent with recent bulk dynamic mechanical analysis results.

Nanoporous gold (NPG), with high specific surface area due to its bicontinuous network of nanometer-sized metallic ligaments and pores, serves as an excellent model system to investigate the influence of surface properties on effective material parameters. For example, the osmotic pressure caused by a charged surface induces larger deformation in the case of a plasma membrane via enhancing the adhesion of Au nanoparticles to the membrane.[1] In continuous metal networks like NPG, the coupling of electric potentials with mechanical stress at the surface results in actuation and sensing capabilities of this class of materials.[2–4] This means the application of an electric potential to NPG will induce a macroscopic strain,[5,6] while the straining of NPG can induce a measurable voltage or current.[4] These functions are inherently mechanically coupled; the amount of actuation for a given potential applied or the strength of the signal sensed for a given applied stress is dependent on the elastic stiffness of the structure. Any possible application of these features requires an appropriate material's strength, and there is a considerable influence of the actuation capability if stress is applied to such an actuator, i.e., if it really has to do work.[7] Therefore, besides the academic interest, the ability to accurately measure mechanical properties and correlate their response to structural characteristics has gained considerable interest in the past 10 years.[7–10]

While the high specific surface is clearly key to the actuation and sensoric functions, it also leads to other effects on mechanical performance not commonly found in conventional bulk systems. When NPG is infiltrated by electrolyte, a certain range of applied potential is able to change the surface state of Au from double-layer capacitance to OH^- adsorption. Such a potential-induced formation of an oxidation monolayer on ligament surface has been found to lead to a twofold increase in strength during the compression of NPG under cycled potential,[11] a reversible response. Sun and Sieradzki observed that this adsorption would not only influence the strength but could also accelerate crack propagation of NPG during dynamic fracture.[12] An improvement of strength and hardness of NPG up to 50% caused by surface modification with self-assembled monolayers was also recently observed.[13,14] It was found that surface tension (i.e., specific surface excess energy) dictates the variation in flow stress under potential control in the capacitive region rather than surface stress.[15] And most interestingly, the extent of the increase in flow stress in all of these cases is dependent on the ligament size,[16] allowing isothermal

annealing of NPG to serve as a tuning parameter for the strength and stiffness coupling for actuation and sensing applications. Yet much debate remains regarding the mechanisms that couple plasticity and electrochemical oxidation adsorption on NPG.

While most investigations of mechanical behavior of NPG are carried out in ambient environments, the few existing electro-chemo-mechanical coupling studies have been carried out on macroscopic samples. Yet a better understanding of the underlying mechanisms controlling the coupled electro-chemo-mechanical response is best achieved via micromechanical testing in an electrochemical cell. Such an approach allows the testing of submicrometer scale volumes, with the possibility to test individual ligaments or load-bearing structural units under electrode potential. By simultaneously changing the surface state of structural elements with their individual surface areas, curvatures, and length-scales, under simultaneous mechanical load, correlations between structure, chemical states, and mechanical response can be investigated. This could provide critical insights needed for the optimization of bicontinuous, nanoporous systems for multifunctional applications. Here, we present such an experimental setup, which allows the mechanical testing of NPG at the microscale in an electrochemical environment.

Nanoindentation, one of the most employed techniques for small scale mechanics, allows us to conduct micromechanical testing under different conditions. A few studies using an AFM-based nanoindentation approach to sharp tip nanoindentation in an electrochemical environment exist. Corcoran *et al.*[17] studied the effect of controlled and reversible oxide or metal monolayer formation on the elastic-plastic transition on planar Au surfaces. The influence of hydrogen on dislocation nucleation during Berkovich indentation was investigated by Barnoush *et al.*,[18] where planar Ni samples were covered by a liquid electrolyte. However, in order to study the stress-strain response of materials undergoing electrochemical driven actuation, the necessary experimental setup is much more challenging.

The appropriate preparation of viable samples for such experiments is itself nontrivial. In typical microcompression experiments,[19] the elastic deformation of the underlying substrate, i.e., the bulk sample from which the micropillar is fabricated, can be readily subtracted from the total measurement using a Sneddon correction.[20] However, in the case of potential-induced actuation experiments, the displacement of the bulk sample induced by the potential cannot be readily subtracted from the measured response. This dictates a need to keep the total bulk sample as thin as possible in order to minimize the bulk displacement or requires a modified loading protocol to circumvent the actuation displacement in the measurement.

Here, disk-shaped NPG samples, manufactured by electrochemical dealloying from $Au_{25}A_{75}$ alloy, with outer dimensions of 2.3 mm diameter and approximately 300 μm thickness, were used for micropillar fabrication. The synthesis process is identical to the corresponding process as described in Ref. 21, and the details can be found in the supplementary material. The average ligament size of our as-dealloyed NPG is around 35 nm, which is quite small compared to the pillar diameter. Thus, no size effects were expected.

After synthesis, the sample was mounted on a SEM stub made of stainless steel. Micropillars with a diameter of 8 μm [see Fig. 1(b)] were milled out of NPG disks by means of focused ion beam (FIB) installed on a FEI Nanolab 200 SEM. The aspect ratio of pillar diameter to height is around 1:3. Axial compression testing of the pillars was

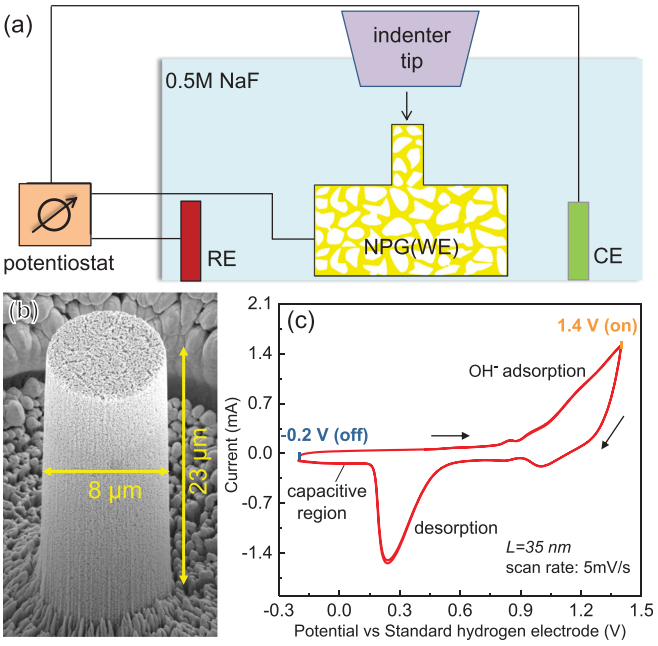

FIG. 1. (a) Schematic diagram of the *in situ* setup for compression tests on micropillars of NPG in the electrolyte where the potential is controlled by a potentiostat. WE: working electrode (NPG); RE: reference electrode (Ag/AgCl); CE: counter electrode (Pt). (b) A SEM image of a 8-micrometer-diameter micropillar with a nominal ligament diameter of 35 nm. (c) Cyclic voltammogram of NPG in 0.5 M-NaF at a scanning rate of 5 mV/s, scan direction as indicated by arrows.

done at a constant strain rate (0.001 s^{-1}) in 0.5 M-NaF on a TI 980 Triboindenter. A conical indenter with a circular flat punch and a nominal diameter of 15 μm fabricated from sapphire was used. As sapphire is an electrical insulator at room temperature, it is highly inert and resistant to chemical attack in most electrochemical environments. A schematic diagram of the electrochemical *in situ* setup is shown in Fig. 1(a). The NPG disk with the milled pillars is placed within an electrochemical cell in a three-electrode setup. NPG serves as working electrode, while a commercially available Ag/AgCl electrode (Driref-2, World Precision Instruments) which is calibrated by a commercial calomel electrode (XR110, Radiometer Analytical) before testing and a platinum wire are used as a reference electrode (RE) and counter electrode (CE), respectively. The three electrodes are connected to a high-performance potentiostat (PG-STAT 302N, Metrohm AUTOLAB) through which the electrode potential applied on the NPG sample is controlled.

Prior to carrying out the microcompression tests under electrochemical control, a cyclic voltammogram is measured to verify a sufficient electrochemical performance of the setup. While most of the macroscopic tests are carried out in $HClO_4$ solution, NaF was preferably used here as to minimize potential damage to the indentation system; NaF has been shown to serve equivalently for actuation of NPG.[22] Only a minimal amount of HF is present in the solution because NaF is a weak base in aqueous solution and tends to remain as F^-, rather than generating a substantial amount of HF. The CV curve presented in Fig. 1(c) was measured at 5 mV/s scan rate in the 0.5 M-NaF electrolyte solution. All electrode potentials in this paper

are specified vs standard hydrogen electrode (SHE). The maximum and minimum potential for the CV scan are 1.4 V and −0.2 V, respectively. The most prominent features of the CV curve are the OH^- adsorption peak associated with the formation of an OH^- monolayer at positive potential and the desorption peak, i.e., the stripping of that monolayer at negative potential. Basing on that, the potential window of adsorption and desorption is recorded, through which we are able to change the surface states by selecting appropriate potentials. From these results, the two potentials, 1.4 V and −0.2 V, which we denote by "on" and "off," respectively, for concision, were then chosen for the *in situ* microcompression experiments, indicating OH^- covered and clean surface, respectively.

Initially a set of pillars were compressed in air as well as in the electrolyte with the constant potential −0.2 V (off) and 1.4 V (on). The results, as exhibited in Fig. 2(a), revealed that engineering stress-strain curves calculated from load-displacement curves measured in air and at −0.2 V using the diameter of the corresponding pillar and correcting for underlying substrate deformation[20,23] are the same, which implies no influence from the infiltration of liquid. The average yield strength, represented by the strength at 2% strain, from 5 micropillars is around 14.78 ± 1.47 MPa in air and 14.87 ± 0.36 MPa at −0.2 V, indicating high reproducibility of the mechanical setup. Multiple partial unloading steps were imposed during the test in order to calculate the elastic modulus at different stages of deformation. There, any given load-unload segment was carried out at a single potential state, i.e., either on or off. In some cases, the entire stress strain curve was measured while the potential was off, others with the potential on, while other set of tests were carried out with intermittent changes in the potential. This allowed the influence of actuation on the displacement and the strength to be decoupled what serves as a major advantage over the previous experiments, where the loading is continuous during potential variation. The flow stress obtained with potential "off" (referring to clean) and "on" (referring to formation of OH^- monolayer) constantly through the whole deformation process is presented in Fig. 2(a) which shows significant differences in behavior under the two kinds of surface states of the nanoscale Au ligaments. The strength increased by 32% when OH^- is adsorbed on the surface, compared to the strength of an identical pillar with a clean surface. This agrees well with the macrocompression results of similar samples in Ref. 11. Multiple partial unloading steps were imposed during the test in order to calculate the elastic modulus at different stages of deformation. There, any given load-unload segment was carried out at a single potential state, i.e., either on or off. Interestingly, the width of the hysteresis loop during the unloading steps increases with increasing strain. The variation of elastic modulus E as calculated from the slope of the initial 20% of data of each unloading curve is illustrated in Fig. 2(b). It is apparent that E increases significantly (from 0.51 ± 0.009 GPa to 3.6 ± 0.017 GPa) during compression largely due to the densification of the sample.[21] Yet an effect of surface adsorption on E is not observed in this experiment; the modulus as a function of strain is identical for both cases of applied potential. The standard deviation of the determined elastic modulus measured from three micropillars at each surface state is less than 2% at all stages of deformation. The precision of the measurement is high enough that a change of the Young's modulus of 8% or more, as reported in Ref. 21, should be clearly discernible. This discrepancy between micro- and macroscale experiments may indicate a history dependence of the mechanism of stiffening, in which the surface state and its possible change with the applied potential depends on its strain path and applied load. It should be noted that the white particles observed on the pillar surface shown in Fig. 2(c) are residual NaF in the crystalline form originating from the electrolyte after drying in air before transferring them into the SEM; it is not related to deformation of the pillar.

The microcompression behavior under potential jumps was also measured in the present study, and the corresponding stress-strain curves are illustrated in Fig. 3. In the case of *in situ* testing, the whole NPG sample is immersed in the electrolyte. Therefore, any actuation resulting from the application of the potential will occur to the whole sample, not just the pillar of interest. Based on the actuation results found in the literature,[2,22] the maximum estimated length change of bulk NPG induced by OH^- adsorption at high potential ranges between 0.03 and 0.1% (mainly depending on the ligament size). This influence of the potential switching, i.e., the actuation of bulk NPG, on the measured displacement is neglected in deformation measurements of bulk samples, but it cannot be ignored in micropillar experiments, in which the displacement due to deformation is concentrated on the pillar but the displacement due to actuation originates from the whole macroscopic sample. Here, five load-unloading cycles are used, shown in Fig. 3(a), each separated by a switching of the applied potential in the unloaded condition. The 1st, 3rd, and 5th cycles were performed at a potential of −0.2 V, while the 2nd and 4th at a potential of 1.4 V, as shown in Fig. 3(b). Schematics of the compression process referring

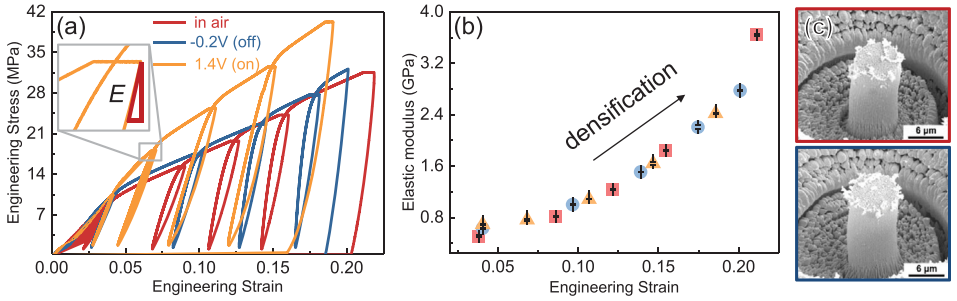

FIG. 2. Results of compression with and without electrolyte in the pores of NPG. (a) Engineering stress-strain curves measured in air and at two constant potentials (1.4 V and −0.2 V) and in 0.5 M-NaF. 1.4 V corresponds to ligament surface covered by OH^- monolayer, while −0.2 V represents a clean surface. (b) The variation of elastic modulus calculated from each unloading curves during compression tests. (c) SEM images of two pillars after compression in air (top) and at −0.2 V (bottom).

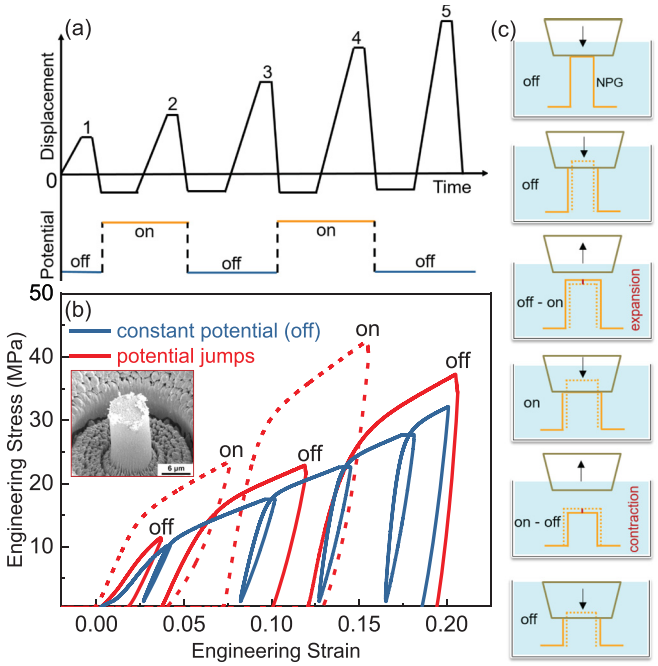

FIG. 3. Results of *in situ* compression under potential jumps. (a) Applied loading profile. (b) Engineering stress-strain curve of pillar under potential jumps (starting with clean surface: off-on-off-on-off) and constant potential (−0.2 V). The inset is the SEM image of pillar after compression under potential jumps. (c) Schematics of compression process under potential jumps refer to the first three loading cycles.

to the first three loading cycles are exhibited in Fig. 3(c). During the first cycle, the displacement grows at the applied constant strain rate until it reaches the set value, holding for 10 s prior to the unloading. After unloading, the flat punch is brought out of contact with the sample surface and held for 40 s, during which we change the potential, here from off (−0.2 V) to on (1.4 V), allowing the expansion of sample to occur without putting additional load on the indenter tip. Then, the next loading cycle is applied on the pillar, and after that the flat punch moves away from the sample surface again, followed by the second switching of the potential from off to on and the induced contraction of the sample before the 3rd loading step. Due to the actuation of the whole sample, the displacement of the flat punch at recontact differs from the last unloading point: during a cycle with the potential at 1.4 V, the indenter contacts the pillar much earlier, i.e., above the last contact point.

The stress-strain curves measured under potential jumps prove that the increase in flow stress upon oxidation of the ligament surface is not based on variations of mechanical properties of different micropillars. The observed variation in flow stress after a potential jump scales with the currently applied stress rather than having a fixed absolute value, in good agreement with macrocompression studies.[11] The SEM images of pillars after compression, in Fig. 2(c) and inset in Fig. 3(b), indicate a uniform deformation in the latter case despite the multiple contacting and change of surface state during testing. Comparison of the flow stress and its changes with applied potential for both presented approaches, constant potential [Fig. 2(a)], and potential jumps [Fig. 3(b)] shows good agreement, suggesting good reproducibility of these measurements.

The electrical resistance of the sample increases by three orders of magnitude when the porous structure is formed during dealloying.[24] However, despite the increase in resistance, we measure smooth and reproducible cyclic voltammogram curves of NPG in the electrolyte [in Fig. 1(c)], and the peaks associated with OH^- adsorption and desorption are clearly observed. Hence, the lowered electrical conductivity does not influence our measurement.

The charging of the surface changes the surface energy and surface stress, and can cause surface adsorption, which leads to the variation of outer dimensions, i.e., actuation, and mechanical performance of NPG simultaneously. The strength of nanoporous micropillars is affected by electrode potential and displays the same trend as the corresponding results of bulk NPG: considerable increase in strength with adsorption and reversible changes with altering surface conditions, while the elastic modulus behaves distinctly: no variation due to surface coverage of OH^-, which is different from the reported behavior of bulk samples in 1 M-$HClO_4$.[21] The sample length-scale, electrolyte, and loading approach used in Ref. 21 are significantly different from that in the present work. The *in situ* compression results of bulk NPG sample in 0.5 M-NaF, as shown in the supplementary material Fig. S1, indicate that a significant influence of the sample size on the change of elastic behavior can be ruled out. The process of electrochemical oxidation of a planar single-crystal Au surface and the effect of specific adsorption of anions (such as SO_4^{2-} and Cl^-) from the electrolyte on the formation of the OH^- monolayer have been investigated thoroughly.[25,26] The F^- and ClO_4^- are two kinds of anions with a strongly bound solvation shell, which induces only weakly specific or even nonspecific adsorption at the gold surface when the NPG is positively charged.[27] We expect that the discrepancy of specific adsorption of F^- and ClO_4^- should be weak compared to the formation of a OH^- monolayer, which dominates the interaction between gold and electrolyte in oxidation region. In order to clarify whether the anion (F^- or ClO_4^-) changes the electro-chemo-mechanical coupling, we carried out macrocompression testing of NPG under potential jumps in 1 M-$HClO_4$ (additionally to the ones in NaF) and presented the results in the supplementary material as Fig. S3. The two potentials 1.5 V (referring to OH^- coverage or oxidized surface) and 0.9 V (referring to the clean surface) vs SHE selected here correspond to the maximum and minimum values of elastic modulus from dynamic mechanical analysis (DMA) results, respectively. Yet the elastic modulus shows no obvious variation at these two different surface states, which agrees well with the *in situ* compression results in 0.5 M-NaF. More likely, this difference is caused by the different loading protocol, i.e., analyzing unloading sections of the stress-strain curve and DMA testing during which the elastic modulus was measured via the analysis of the oscillatory load and displacement signals by a lock-in amplifier while the potential was changed. The load state can have a strong influence on the variation of mechanical properties during the change of electrode potential for nanoporous metals.[28] This points to the advantage of this microscale test setup which allows the decoupling of the actuation and loading responses.

NPG wetted in the electrolyte will show local inhomogeneities on a short time scale when the potential is changed, specifically from capacitive to oxidation regimes. The concentration gradient of ions exists within the pores due to the formation of the OH^- monolayer on the ligament surface, which in turn induces ion movement between the outer and inner (pores) electrolyte. In our *in situ* experiments, as

shown by the current-time curves in the supplementary material Fig. S4, the current reaches a steady state in a time of about 45 s after a potential change due to the high mobility of the ions in solution. In the case of the microcompression experiments, the NPG (sample and substrate) has sufficient time to recover a homogeneous state after the potential jump before the next loading segment is applied. In the case of the macrocompression experiments shown in the supplementary material, a very low applied strain rate of only $0.0001\,s^{-1}$ is applied which is by orders of magnitude slower than the charging process.

In conclusion, *in situ* microcompression testing of NPG in an electrolyte under potential control provides critical opportunities to investigate the influence of microstructural aspects on the electro-chemo-mechanical coupling. By using a multiple load-unload profile for *in situ* compression under potential control, we were able to decouple the actuation effect from the impact of elastic strain when the potential changes. The microcompression results herein show a similar effect of surface conditions on plastic behavior as observed in bulk compression of NPG; the strength increased with increased surface coverage of OH^- and showed recoverable modulation with varying surface states. However, the change in surface states as achieved with applied potential in the case of microcompression did not lead to an increase in stiffness as described in the literature for macroscale tests. Finally, through the demonstrated robustness of this approach to investigate electro-chemo-mechanical coupling at the microscale, the influence of single ligaments, grain boundaries, or other structural elements can be investigated. In turn, this could lead to the exploitation of structural anisotropy for functional response of bicontinuous nanoporous materials.

See the supplementary material for more details on the synthesis process of NPG and the results of *in situ* macrocompression experiments on bulk NPG in 0.5 M-NaF as well as in 1 M-$HClO_4$.

This work was funded by the Deutsche Forschungsgemeinschaft (DFG, German Research Foundation)-Projektnummer 192346071-SFB 986. The authors would like to thank Jie Li for helping in $Au_{25}Ag_{75}$ alloy preparation.

REFERENCES

[1]S. Sinha, H. Jing, H. S. Sachar, and S. Das, Appl. Phys. Lett. **112**, 163702 (2018).
[2]H.-J. Jin, X.-L. Wang, S. Parida, K. Wang, M. Seo, and J. Weissmüller, Nano Lett. **10**, 187 (2010).
[3]J. Weissmüller, R. N. Viswanath, D. Kramer, P. Zimmer, R. Würschum, and H. Gleiter, Science **300**, 312 (2003).
[4]C. Stenner, L. Shao, N. Mameka, and J. Weissmüller, Adv. Funct. Mater. **26**, 5174 (2016).
[5]D. Kramer, R. N. Viswanath, and J. Weissmüller, Nano Lett. **4**, 793 (2004).
[6]H.-J. Jin and J. Weissmüller, Adv. Eng. Mater. **12**, 714 (2010).
[7]L.-Z. Liu, X.-L. Ye, and H.-J. Jin, Acta Mater. **118**, 77 (2016).
[8]K. Hu, M. Ziehmer, K. Wang, and E. T. Lilleodden, Philos. Mag. **96**, 3322 (2016).
[9]X.-Y. Sun, G.-K. Xu, X. Li, X.-Q. Feng, and H. Gao, J. Appl. Phys. **113**, 023505 (2013).
[10]M. Hakamada and M. Mabuchi, Scr. Mater. **56**, 1003 (2007).
[11]H.-J. Jin and J. Weissmüller, Science **332**, 1179 (2011).
[12]S. Sun, X. Chen, N. Badwe, and K. Sieradzki, Nat. Mater. **14**, 894 (2015).
[13]N. Mameka, L. Lührs, S. Heissler, H. Gliemann, and C. Wöll, ACS Appl. Nano Mater. **1**, 6613 (2018).
[14]N. Miyazawa, J. Ishimoto, M. Hakamada, and M. Mabuchi, Appl. Phys. Lett. **109**, 261905 (2016).
[15]N. Mameka, J. Markmann, and J. Weissmüller, Nat. Commun. **8**, 1976 (2017).
[16]P. Wu, X.-L. Ye, L.-Z. Liu, and H.-J. Jin, Mater. Res. Lett. **6**, 508 (2018).
[17]S. G. Corcoran, S. R. Brankovic, N. Dimitrov, and K. Sieradzki, Mat. Res. Soc. Symp. Proc. **505**, 77 (1998).
[18]A. Barnoush, J. Dake, N. Kheradmand, and H. Vehoff, Intermetallics **18**, 1385 (2010).
[19]E. Lilleodden, Scr. Mater. **62**, 532 (2010).
[20]I. N. Sneddon, Int. J. Eng. Sci. **3**, 47 (1965).
[21]N. Mameka, J. Markmann, H.-J. Jin, and J. Weissmüller, Acta Mater. **76**, 272 (2014).
[22]L.-H. Shao, H.-J. Jin, R. N. Viswanath, and J. Weissmüller, Europhys. Lett. **89**, 66001 (2010).
[23]C. A. Volkert and E. T. Lilleodden, Philos. Mag. **86**, 5567 (2006).
[24]E.-M. Steyskal, M. Seidl, M. Graf, and R. Würschum, Phys. Chem. Chem. Phys. **19**, 29880 (2017).
[25]H. Angerstein-Kozlowska, B. Conway, A. Hamelin, and L. Stoicoviciu, J. Electroanal. Chem. Interfacial Electrochem. **228**, 429 (1987).
[26]H. Angerstein-Kozlowska, B. Conway, B. Barnett, and J. Mozota, J. Electroanal. Chem. Interfacial Electrochem. **100**, 417 (1979).
[27]O. Magnussen, Chem. Rev. **102**, 679 (2002).
[28]L.-Z. Liu, N. Mameka, J. Markmann, H.-J. Jin, and J. Weissmüller, Phys. Rev. Mater. **3**, 066001 (2019).